

1 **Interferon signaling suppresses the unfolded protein response and induces cell death in**
2 **hepatocytes accumulating hepatitis B surface antigen**

3

4 Short title: IFNs induce cell death in hepatocytes accumulating hepatitis B surface antigen

5 Ian Baudi^{1¶}, Masanori Isogawa^{1,2¶*}, Federica Moalli³, Masaya Onishi^{1,4}, Keigo Kawashima^{1,5},
6 Yusuke Sato⁶, Hideyoshi Harashima⁶, Hiroyasu Ito⁷, Tetsuya Ishikawa⁸, Takaji Wakita⁹,
7 Matteo Iannacone³, and Yasuhito Tanaka^{1,10*}

8

9 ¹ Department of Virology and Liver Unit, Nagoya City University Graduate School of
10 Medical Sciences, Nagoya, Japan

11 ² Department of Immunology, National Institute of Infectious Diseases, Tokyo, Japan

12 ³ Division of Immunology, Transplantation, and Infectious Diseases, IRCCS San Raffaele
13 Scientific Institute, Milan, Italy.

14 ⁴ Department of Gastroenterology/Internal Medicine, Gifu University Graduate School of
15 Medicine, Gifu, Japan

16 ⁵ Department of Gastroenterology and Hepatology, Yokohama City University School of
17 Medicine, Yokohama, Japan.

18 ⁶ Laboratory of Innovative Nanomedicine, Faculty of Pharmaceutical Sciences, Hokkaido
19 University, Sapporo, Japan.

20 ⁷ Department of Joint Research Laboratory of Clinical Medicine, Fujita Health University
21 School of Medicine, Toyoake, Japan.

22 ⁸ Department of Radiological and Medical Laboratory Sciences, Nagoya University Graduate
23 School of Medicine, Nagoya, Japan.

24 ⁹ National Institute of Infectious Diseases, Tokyo, Japan.

25 ¹⁰ Department of Gastroenterology and Hepatology, Faculty of Life Sciences, Kumamoto
26 University, Kumamoto, Japan.

27

28

29 *Corresponding authors

30 E-mail: nisogawa@niid.go.jp (MI)

31 E-mail: ytanaka@kumamoto-u.ac.jp (YT)

32

33 ¶These authors contributed equally to this work.

34

35 Coauthors E-mail addresses

36 Ian Baudi: baudiian@gmail.com

37 Federica Moalli: moalli.federica@hsr.it

38 Masaya Onishi: om19840905@gmail.com

39 Keigo Kawashima: keepitgood0110@yahoo.co.jp

40 Yusuke Sato: y_sato@pharm.hokudai.ac.jp

41 Hideyoshi Harashima: harasima@pharm.hokudai.ac.jp

42 Hiroyasu Ito: hiroyasu.ito@fujita-hu.ac.jp

43 Tetsuya Ishikawa: ishikawa@met.nagoya-u.ac.jp

44 Takaji Wakita: wakita@niid.go.jp

45 Matteo Iannacone: iannacone.matteo@hsr.it

46

47 **Abstract**

48 Virus infection, such as hepatitis B virus (HBV), often causes endoplasmic reticulum (ER)
49 stress. The unfolded protein response (UPR) is counteractive machinery to ER stress, and the
50 failure of UPR to cope with ER stress results in cell death. Mechanisms that regulate the
51 balance between ER stress and UPR in HBV infection is poorly understood. Type 1 and type
52 2 interferons have been implicated in hepatic flares during chronic HBV infection. Here, we
53 examined the interplay between ER stress, UPR, and IFNs using transgenic mice that express
54 hepatitis B surface antigen (HBsAg) (HBs-Tg mice) and humanized-liver chimeric mice
55 infected with HBV. IFN α causes severe and moderate liver injury in HBs-Tg mice and HBV
56 infected chimeric mice, respectively. The degree of liver injury is directly correlated with
57 HBsAg levels in the liver, and reduction of HBsAg in the transgenic mice alleviates IFN α
58 mediated liver injury. Analyses of total gene expression and UPR biomarkers' protein
59 expression in the liver revealed that UPR is induced in HBs-Tg mice and HBV infected
60 chimeric mice, indicating that HBsAg accumulation causes ER stress. Notably, IFN α
61 administration transiently suppressed UPR biomarkers before liver injury without affecting
62 intrahepatic HBsAg levels. Furthermore, UPR upregulation by glucose-regulated protein 78
63 (GRP78) suppression or low dose tunicamycin alleviated IFN α mediated liver injury. These
64 results suggest that IFN α induces ER stress-associated cell death by reducing UPR. IFN γ
65 uses the same mechanism to exert cytotoxicity to HBsAg accumulating hepatocytes.
66 Collectively, our data reveal a previously unknown mechanism by which IFNs selectively
67 induce cell death in virus-infected cells. This study also identifies UPR as a potential target
68 for regulating ER stress-associated cell death.

69

70

71 **Author summary**

72 Hepatitis B virus (HBV) causes acute and chronic infections that kill over 600,000 people
73 every year from severe hepatitis, liver cirrhosis, and cancer. Mechanisms of chronic liver
74 injury remain largely unknown. Both type 1 and type 2 interferons (IFNs) have been
75 implicated in hepatic flares during chronic HBV infection, although HBV per se is a poor
76 IFN inducer. In addition, while IFN α , a type 1 IFN, used to be the first-line treatment for
77 chronic hepatitis B (CHB) patients, adverse side effects, including hepatic flares, severely
78 limit their therapeutic effectiveness. These clinical observations suggest a pathogenic role of
79 IFNs in HBV infection. Here, we demonstrate that IFN-1s cause severe and moderate
80 hepatitis in transgenic mice expressing hepatitis B surface antigen (HBs-Tg mice) and human
81 hepatocyte chimeric mice infected with HBV, respectively. HBsAg accumulation appears to
82 cause ER stress because a counteractive response to ER stress, namely, unfolded protein
83 response (UPR), was induced in both HBs-Tg mice and HBV infected chimeric mice. Our
84 results indicate that IFN-1s suppress UPR before causing liver injury. UPR was also
85 suppressed by IFN γ . Induction of UPR in HBs-Tg mice before treatment with IFN α and IFN γ
86 significantly alleviated liver injury. We suggest that IFNs exert cytotoxicity to ER stress
87 accumulating cells by suppressing UPR.

88

89 **Keywords**

90 Interferons, ER stress, unfolded protein response, cell death, hepatitis B virus, surface
91 antigen, liver injury

92 **Introduction**

93 Interferons (IFNs) play a critical role in host defense against pathogens, particularly
94 viruses, by activating the expression of hundreds of genes that exert antiviral activity [1].
95 IFNs also cause immunopathology during viral infections [2,3]. The basis behind the IFN-
96 mediated immunopathology has yet to be fully elucidated but appears to include
97 phosphorylation of eukaryotic initiation factor-2 α (eIF-2 α), activation of RNase L, and
98 induction of nitric oxide synthase (iNOS) [1,2]. Little is known about whether and how
99 infected cells are preferentially sensitized to IFN-mediated cell death.

100 The endoplasmic reticulum (ER) is responsible for much of a cell's protein synthesis
101 and folding. An imbalance between the protein-folding load and the capacity of the ER
102 causes unfolded or misfolded proteins to accumulate in the ER lumen, resulting in ER stress
103 [4,5]. To cope with ER stress, a protective mechanism called the unfolded protein response
104 (UPR) is activated to reduce protein synthesis and/or enhance degradation, folding, and
105 secretion of the offending proteins [4,5]. UPR has been linked to various pathological states,
106 including malignancies, neurodegenerative, storage, metabolic, and infectious diseases [6–
107 11]. While unmitigated ER stress leads to cell death [12], it is unclear whether the
108 concomitant UPR plays a pro- or anti-cell survival role in such cases. Maladaptation of UPR
109 as the underlying pathogenic mechanism has been poorly studied, particularly in highly
110 secretory organs such as the liver and pancreas that are prone to ER stress [13]. Although
111 infections with several viruses have been reported to induce ER stress [14–19], the interplay
112 between ER stress, UPR, and IFN signaling has not been adequately interrogated.

113 Hepatitis B virus (HBV) causes acute and chronic liver disease. Patients with chronic
114 hepatitis B (CHB) often experience hepatic flares in association with hepatitis B surface
115 antigen (HBsAg) accumulation [20,21]. Factors that cause hepatic flares in CHB patients are

116 incompletely understood. IFN α , a type-1 IFN (IFN-1), is widely used as the first-line drug
117 for the treatment of chronic hepatitis B (CHB) [22]. High serum IFN α levels have been
118 reported in some CHB patients experiencing spontaneous hepatic flares [23] or antiviral
119 therapy withdrawal-associated hepatic flares [24]. However, the molecular mechanisms
120 behind the IFN-1 related liver injury largely remain obscure. In addition, CXCL10, an IFN γ
121 inducible chemokine, has been associated with disease progression [25] as well as HBsAg
122 clearance in CHB patients [26]. In this study, we examined the role of IFNs in liver injury
123 associated with ER stress using transgenic mice that express HBsAg in the liver (HBs-Tg
124 mice) and HBV-infected humanized-liver chimeric mice. Our data suggest that IFNs
125 selectively causes cell death in hepatocytes under ER stress by perturbing UPR.

126 **Results**

127 **Type-1 IFNs induce liver injury in association with HBsAg-retention.**

128 To investigate the role of IFN-1 signaling in liver injury associated with intrahepatic
129 HBsAg accumulation, we used HBs-Tg mice (lineage 107-5D) that produce HBsAg [27].
130 Groups of 3-4 HBs-Tg mice or their non-transgenic littermates (WT) were intravenously
131 injected with the IFN-1 inducer poly I:C or saline. Liver injury was monitored by measuring
132 serum ALT activity (sALT) on days 1, 3, and 7 after treatment. As shown in Fig 1A, sALT
133 was markedly elevated in the HBs-Tg mice, peaking on day 1 after poly I:C treatment, but
134 not in the WT mice. We also examined whether poly I:C treatment could induce sALT
135 elevation in HBV-replication-competent transgenic (HBV-Tg) mice (Lineage 1.3.32) [28].
136 As shown in Fig 1B, HBV-Tg mice readily secrete HBsAg, retaining approximately 100-fold
137 less HBsAg in the liver compared with the HBs-Tg mice. Interestingly, no ALT elevation
138 occurred in the HBV-Tg mice after poly I:C treatment (Fig 1C). Taken together, these results
139 suggest that poly I:C-induced liver injury is associated with marked intrahepatic HBsAg
140 accumulation.

141 **Fig 1. Poly I:C induces liver injury in association with HBsAg-retention.** (A) Serum
142 ALT levels measured on days 0, 1, 3, and 7 after PBS (white bars) or poly I:C (10 μ g) (red
143 bars) treatment in HBs-Tg mice (left graph) and WT mice (right graph). (B) Comparison of
144 HBsAg expression levels between HBs-Tg (Lineage 107-5D: white bars) and HBV-Tg mice
145 (Lineage 1.3.32: grey bars) in the serum (left graph) and the liver (right graph). (C) Serum
146 ALT levels in HBs-Tg mice and HBV-Tg mice 24 hours after intravenous injection of PBS or
147 poly I:C. Mean values \pm s.d of pooled data from 3 independent experiments are shown.

148

149 To examine the role of IFN-1 signaling in the poly I:C induced liver injury in HBs-Tg
150 mice, groups of HBs-Tg mice (n=4) were treated with anti-IFN α / β receptor 1 (IFN α β R1)
151 antibody that blocks IFN-1 signaling or a control antibody and then injected with poly I:C 24
152 hours later. The impact of IFN-1 signaling blockade was evaluated by monitoring sALT
153 activity. As shown in Fig 2A, anti-IFN α β R1 antibody but not the control antibody treatment
154 prevented sALT elevation, indicating that the liver injury induced after poly I:C treatment in
155 HBs-Tg mice was dependent on IFN-1 signaling. To confirm that IFN-1 induces liver injury,
156 groups of HBs-Tg mice (n=3) and control mice (n=3) were intravenously injected with 5
157 million units (MU)/kg of recombinant mouse IFN α , and sALT was monitored on days 1, 3,
158 and 7. As expected, IFN α induced sALT elevation in the HBs-Tg mice, peaking on day 1 and
159 receding towards baseline on day 3. No sALT elevation occurred in the normal mice (Fig
160 2B). Interestingly, liver immunohistochemical analysis showed almost no inflammatory cell
161 infiltration at 24 hours despite severe sALT elevation, suggesting a sterile nature of IFN α
162 mediated cell-death (Fig 2C). When apoptosis was examined by TUNEL staining at 16 hours
163 after IFN α , a relatively small fraction of TUNEL positive hepatocytes were found scattered
164 throughout the parenchyma (Fig 2D).

165 **Fig 2. IFN-1s trigger HBsAg-associated liver injury in the absence of inflammatory cell**
166 **infiltration.** (A) Isotype control antibodies (250 μ g; red bars) or anti-IFN α β R1 (250 μ g;
167 black bars) were intraperitoneally injected into HBs-Tg mice (n=3-4) 24 hours before poly
168 I:C treatment. ALT levels on days 0, 1, 3, and 7 after poly I:C treatment are shown. (B)
169 Serum ALT values in HBs-Tg (left graph) and WT mice (right graph) on days 0, 1, 3, and 7
170 after intravenous injection of PBS (white bars) or IFN α (5 million units (MU)/kg; blue bars).
171 (C) Histological characteristics after IFN α injection in HBs-Tg mice. The panels show
172 representative Hematoxylin and Eosin staining at 24 hours after IFN α . (D) TUNEL staining

173 at 16 hours after IFN α treatment. The arrows show representative apoptotic cells in HBs-Tg
174 mice.

175

176 To examine the impact of HBsAg reduction on IFN-mediated liver injury, HBs-Tg
177 mice were injected by siRNA targeting HBV (siHBV) that were shown to reduce HBV
178 mRNA in HBV-infected human hepatocyte chimeric mice [29,30] or control siRNA, and
179 then intrahepatic HBsAg and HBV mRNA levels were determined 4 days later (S1A Fig). As
180 shown in S1B Fig, siHBV had no discernable effect on HBsAg, although it strongly
181 suppressed HBV mRNA expression (S1C Fig), indicating the stable nature of intracellular
182 HBsAg. To induce hepatocyte turnover, we adoptively transferred HBsAg-specific T-cells
183 that were shown to induce severe hepatitis in HBs-Tg mice [31] to groups of HBs-Tg mice
184 (n=4) seven days before injecting siHBV or siControl. As shown in Fig 3B, HBsAg was
185 significantly reduced on day 7 after siHBV treatment when hepatocyte turnover was
186 previously induced. These mice were then injected intravenously with recombinant mouse
187 IFN α on day 7 after siHBV treatment. A day after IFN α injection (day 8), serum ALT levels
188 were significantly reduced in siHBV treated mice compared with their siControl treated
189 littermates (sALT 425 \pm 103 vs. 4227 \pm 2533, p=0.027) (Fig 3C). These results indicate that
190 IFN α mediated liver injury can be prevented by the reduction of intrahepatic HBsAg levels.

191 **Fig 3. Reduction of intrahepatic HBsAg alleviates IFN mediated liver injury. (A)**

192 Experimental design. HBs-Tg mice were adoptively transferred with HBsAg-specific effector
193 CD8 T cells on day 7 day before siRNA treatment. On day 7 after siRNA treatment, mice
194 were intravenously injected with IFN α (5 MU/kg) and, on day 8, monitored for sALT levels.

195 (B) Suppression of intrahepatic HBsAg expression before IFN α treatment (day 7 after siRNA
196 treatment). (C) Serum ALT levels before (day 7) and after (day 8) IFN α treatment.

197

198 **IFN-1 signaling perturbs UPR in association with liver injury in HBs-Tg mice.**

199 To elucidate the molecular mechanism by which IFN-1 induces liver injury in HBs-
200 Tg mice, we serially profiled the liver transcriptomes of both HBs-Tg and control mice
201 treated with IFN α by microarray analyses. We especially searched for distinct genes whose
202 expression correlated with the IFN α mediated liver injury in HBs-Tg mice. To do so, snap-
203 frozen liver samples were obtained from groups of four HBs-Tg and control mice sacrificed
204 prior to (0 hour) and 2, 4, 8, and 24 hours after treatment with 5 MU/kg of IFN α or vehicle.
205 Liver injury progression was also monitored at these time points using sALT. As shown in
206 Fig 4A, a significant sALT increase was observed in HBs-Tg mice from 8 hours post-IFN
207 treatment and peaked at 24 hours (3758 ± 649 U/L). As expected, no sALT elevation
208 occurred in the WT mice. Cluster and enrichment analyses were performed on the
209 microarray data for the selected period prior and up to the onset of liver injury, i.e., 0, 2, 4,
210 and 8-hour time-points. As shown in Figs 4B and 4C, six clusters showing distinct gene
211 expression profiles were identified. Many ISGs could be found in TLR signaling and
212 chemokine signaling pathways of Cluster 6 (Fig 4C), which were induced similarly between
213 HBs-Tg and WT mice (Figs 4B and 4C). Cluster 3 genes were upregulated in HBs-Tg mice
214 before IFN treatment, and as ISGs were induced, they were downregulated in both HBs-Tg
215 and WT mice up to 4 hours (Fig 4B), suggesting a suppressive effect of ISGs on these genes.
216 Interestingly, while the expression of these genes rebounded in WT mice, they remained
217 downregulated in HBs-Tg mice at 8 hours after IFN treatment. Importantly, Cluster 3
218 includes genes related to protein processing in the endoplasmic reticulum (Fig 4C), raising

219 the possibility that IFN α induced liver injury in HBs-Tg mice by modulating intrahepatic
220 UPR. To test this, the correlation between liver injury, IFN-1 signaling, and UPR-related
221 molecule expression was further examined. Intrahepatic induction of interferon-stimulated
222 genes (ISGs), UPR biomarkers such as spliced X-box binding protein-1 (XBP1s)
223 phosphorylated- PKR-like ER kinase (phos-PERK) and C/EBP homologous protein (CHOP)
224 (Fig 4D) were assessed by western blot. As shown in S2A Fig, non-treated HBs-Tg mice
225 showed higher baseline expression of XBP-1s, phos-PERK, and CHOP in association with
226 moderate liver injury (sALT 100-300 U/L) than non-treated WT mice (S2B Fig), suggesting
227 that HBsAg accumulation triggered UPR activation in association with mild spontaneous
228 hepatitis. Interestingly, as shown in Fig 4E, the expression of XBP1-s and phos-PERK were
229 transiently suppressed during ISG induction, in concordance with the mRNA levels
230 represented in Cluster 3 of the microarray data (Figs 4B and 4C). As XBP1s and phos-PERK
231 returned towards baseline levels, CHOP began to increase markedly in HBs-Tg mice from 8
232 hours and peaked at 24 hours in direct correlation with sALT. An ER chaperone molecule,
233 glucose-regulated protein 78 (GRP78) was also upregulated in HBs-Tg mice at 24hours (Fig
234 4E), in association with peak liver injury (Fig 4A). The aforementioned changes were not
235 observed in WT mice, although XBP1 expression was modestly reduced immediately after
236 IFN α treatment (Fig 4E). These data suggest that IFN-signaling induces liver injury in HBs-
237 Tg mice in association with UPR modulation.

238 **Fig 4. IFN-1 signaling perturbs UPR in association with liver injury in HBs-Tg mice.**

239 (A) Liver injury progression after IFN α treatment. The graph shows sALT levels in WT
240 mice (white bars) and HBs-Tg mice (black bars) after IFN α treatment (5MU/kg). Mean
241 values +/- s.d of pooled data from 3 independent experiments are shown. (B) Differentially
242 expressed genes (DEGs) in the microarray data of HBs-Tg and WT mice after IFN α
243 treatment. Each of the 6 graphs shows a distinct cluster identified using microarray time-

244 course-specific maSigPro [32] software. (C) List of gene pathways selectively enriched in the
245 6 clusters. (D) A schematic diagram showing simplified unfolded response pathways. (E)
246 Representative immunoblots showing UPR-biomarker protein expression in HBs-Tg mice
247 (left panel) and WT mice (right panel) at specified time points after IFN α treatment.

248

249 **IFN α induces liver injury in HBV infected human chimeric mice in association with**
250 **XBP1 suppression.**

251 To examine the effect of IFN α treatment on UPR in HBV infected human liver, we
252 used human liver chimeric mice, i.e., uPA-SCID mice whose livers had been repopulated
253 with human hepatocytes as previously described [33]. We first compared circulating and
254 intracellular HBsAg levels between HBV-Tg mice, HBs-Tg mice, and chimeric mice infected
255 with HBV for 6 weeks. As shown in S3 Fig, HBV infected chimeric mice secreted more
256 HBsAg than HBV-Tg mice (>10-fold difference) and HBs-Tg mice (>100-fold difference)
257 (S3A Fig) but still retained more HBsAg in the liver than 1.3.32 HBV-Tg mice (S3B Fig).
258 Next, groups of nine chimeric mice were infected with HBV (genotype C isolate,
259 C2_JPNAT, from a chronic HBV patient[33]), and after the establishment of persistent
260 infection (6-8 weeks after HBV inoculation), the mice were intravenously administered with
261 25 ng/g of pegylated-human IFN α (PEG-hIFN α), and then sacrificed after 8 and 24 hours
262 (n=3 per group) (Fig 5A) to examine the correlation between liver injury (sALT) (Fig 5B),
263 IFN-1 signaling, and UPR-related molecules measured by quantitative-PCR (Fig 5C) and
264 western blot (Fig 5D). Non-infected, non-treated control chimeric mice (n=2) were also
265 sacrificed and included in the analyses. Before PEG-hIFN α treatment, HBV infected
266 chimeric mice showed slightly higher sALT activity than untreated mice (Fig 5B, mean 268
267 vs. 130 U/L, p=0.001) in association with modest intrahepatic upregulation of UPR

268 molecules including XBP1s and PERK (Fig 5C). Importantly, sALT levels increased in HBV
269 infected chimeric mice at 8 (724 ± 159 U/L) and 24 hours (616 ± 26 U/L) after PEG-hIFN α
270 treatment (Fig 5B) in association with an increased level of ISG15 expression and reduced
271 levels of UPR-related molecules compared to non-treated HBV infected mice (Fig 5C and
272 5D). Intracellular HBsAg levels were mostly unchanged during the 24-hour period (Fig 5D),
273 suggesting that the suppression of UPR-related molecules, including XBP1s, was not due to a
274 reduction of HBV surface antigens. Collectively, these results indicate that bona fide HBV
275 infection could induce UPR in human hepatocytes, and IFN-1 signaling induces liver injury
276 in association with UPR suppression.

277 **Fig 5. IFN α induces liver injury in HBV infected human chimeric mice in association**
278 **with XBP1 suppression.** (A) Experimental design. HBV infected mice were injected with 25
279 ng/g pegylated IFN α -2a and then sacrificed at specified time points (n=3 per time point). (B)
280 Liver injury after IFN treatment in HBV infected chimeric mice. The graph shows serum
281 ALT levels at baseline (0 h), 8, and 24 hours after IFN treatment (black bars) compared with
282 non-infected non-treated chimeric mice (white bars). Data are shown as mean values +/- s.d.
283 (C) Messenger RNA expression levels of UPR biomarkers after IFN treatment. Levels of
284 UPR related molecule mRNA expression determined by quantitative PCR. (D) Association
285 between XBP, ISG15, and HBV surface antigen (HBsAg) after IFN treatment.
286 Representative immunoblots showing UPR biomarkers XBP1, ISG15, and HBsAg levels at
287 0, 8, and 24 hours after IFN treatment.

288

289 **IFNs exert direct cytotoxicity to HBsAg accumulating hepatocytes and downregulate**
290 **UPR.**

291 To dissect the mechanism of the IFN α -mediated liver injury, we established a
292 primary mouse hepatocyte (PMH) culture system amenable to knockdown experiments.
293 Primary hepatocytes from both HBs-Tg and WT mice were treated with IFN α or medium,
294 and then cytotoxicity and UPR-related protein expression were assessed 8, 24, and 72 hours
295 later (Fig 6A). The degree of cytotoxicity was analyzed by calculating the percentage of
296 specific cell death based on LDH activity in the supernatant as described in the Materials and
297 Methods. As shown in Fig 6B, cytotoxicity was clearly observed at 72 hours after IFN α
298 treatment in the HBs-Tg PMHs but not in the WT PMHs, indicating that IFN α is directly and
299 specifically cytotoxic to HBsAg accumulating hepatocytes. Interestingly, UPR markers such
300 as XBP1s, phosho-PERK, and CHOP expression were upregulated from 24 hours, and then
301 diminished at 72 hours coinciding with ISG induction and cytotoxicity. Furthermore, GRP78
302 was upregulated at 72 hours in association with cytotoxicity. No UPR modulation was
303 observed in the WT PMHs (Fig 6C). These in vitro data closely recapitulate our observations
304 in vivo despite the slower temporal dynamics of ISG induction in vitro and lower baseline
305 UPR in HBsAg PMHs. To determine whether the observed suppressive effect of IFN α on
306 UPR was a general occurrence or restricted to the HBs-Tg model, we tested the impact of
307 IFN-1 signaling on UPR that was chemically induced by thapsigargin in normal PMHs at 6
308 and 12 hours (Fig 6D). Interestingly, thapsigargin-induced Perk and CHOP but not XBP1s
309 expression were clearly suppressed by IFN α treatment at both time points (Fig 6E),
310 suggesting that UPR suppression by IFN α was in part a general phenomenon.

311 **Fig 6. IFN α exerts direct cytotoxicity to HBsAg accumulating hepatocytes and**
312 **downregulate UPR.** (a-c) Effects of IFN signaling and UPR modulation on HBsAg
313 accumulating hepatocytes in vitro. (A) Experimental design. (B) LDH levels in the
314 supernatant of PMH culture were measured at indicated time points after adding medium

315 (white bars) or IFN α (0.1MU/ml) (black bars). (C) The immunoblots of UPR related
316 molecules and ISG15 at specified time points after IFN α treatment. (D, E) IFN α suppresses
317 chemically induced UPR in vitro. (D) Experimental schema. (E) Representative
318 immunoblots show the effect of IFN α on UPR related-protein levels at 0, 6, and 12 hours
319 after treatment with thapsigargin.

320

321 We also tested the direct effect of IFN γ on hepatocytes accumulating HBsAg using
322 the previously described in-vitro culture system (S4A Fig), because IFN γ has been reported
323 to induce liver injury in mice that retain HBsAg in the liver [31,34]. As expected, IFN γ
324 (10,000 U/ml) directly and specifically induced cell death in HBs-Tg PMHs (S4B Fig).
325 Again, UPR was upregulated at 24 hours and then downregulated at 72 hours in association
326 with cytotoxicity and GRP78 upregulation (S4C Fig), similar to IFN α .

327 **GRP78 suppression reduces IFN-induced hepatocytotoxicity by upregulating UPR.**

328 To determine the role of UPR related molecules in IFN α -mediated
329 hepatocytotoxicity, CHOP, GRP78 and XBP1 were downregulated by transfecting HBs-Tg
330 PMHs with target-specific siRNA or a scrambled siRNA control for 24 hours before addition
331 of IFN α (Fig 7A). Cytotoxicity was assessed by measuring secreted LDH levels in culture
332 supernatants 72 hours after IFN α addition. Surprisingly, suppression of GRP78 but not
333 CHOP or XBP1 reduced LDH (Fig 7B) in association with upregulation of UPR related
334 molecules, including PERK and XBP1s (Fig 7C). To determine whether the reduction in
335 IFN α cytotoxicity by siGRP78 was due to the UPR upregulation, GRP78 and the key UPR
336 molecule XBP1 were co-suppressed prior to IFN α treatment. Interestingly, the reduction of

337 cytotoxicity by siGRP78 was lost when XBP1 was co-suppressed (Figs 7D and 7E),
338 suggesting that UPR is required for the reduction of cytotoxicity by GRP78 suppression.
339 These results suggest that robust UPR activation by GRP78 suppression rescues HBsAg
340 accumulating hepatocytes from the cytotoxic effect of IFN α .

341 **Fig 7. GRP78 suppression reduces IFN α -induced hepatocytotoxicity in association with**
342 **UPR upregulation.** (A) Experimental design. Small interfering RNA (siRNA) targeting
343 CHOP, GRP78, XBP1, or control scramble siRNA (siControl) (15 μ M) were transfected to
344 primary mouse hepatocytes (PMHs) from HBs-Tg and WT mice before IFN α treatment. (B)
345 LDH levels in the supernatant of cultured HBs-Tg PMHs after IFN α treatment following
346 knockdown of each UPR-related molecule by specific siRNA. (C) Representative
347 immunoblots showing UPR-related protein levels in the absence/presence of IFN α after
348 indicated specific target downregulation by siRNA. (D) LDH levels in the supernatant of
349 cultured HBs-Tg PMHs after IFN treatment following control, GRP78, and GRP78/XBP1 co-
350 suppression by siRNA. (E) UPR-related protein levels in the absence/presence of IFN α in
351 siControl, siGRP78, and siGRP78/siXBP1 suppressed HBs-Tg PMHs. Mean values \pm s.d of
352 pooled data from 2 independent experiments are shown.

353

354 **UPR upregulation alleviates IFN-induced liver injury in HBs-Tg mice.**

355 To determine whether GRP78 suppression could alleviate liver injury in HBs-Tg
356 mice, we intravenously injected siRNA targeting GRP78 (siGRP78), or control siRNA, into
357 groups of 3-4 HBs-Tg mice 4 days before IFN α treatment (Fig 8A). As shown in Fig 8B,
358 siGRP78 treated mice exhibited 3-5-fold lower sALT levels after IFN α treatment compared
359 to control siRNA treated mice (mean 7110 ± 42 U/L vs. 1610 ± 794 U/L, $p=0.003$). These

360 data suggest that robust UPR induction prevents IFN-induced liver injury in HBs-Tg mice.
361 Therefore, the impact of UPR augmentation on IFN-mediated liver injury was tested using a
362 chemical UPR inducer, tunicamycin. Groups of HBs-Tg and WT mice (n=3) were
363 intraperitoneally injected with a low dose of tunicamycin (0.1 mg/kg) or saline. Significant
364 UPR upregulation could be seen 4 hours after tunicamycin treatment (Fig 8C), at which time
365 point IFN α (5 MU/kg) or 50 ng α -Galactosylceramide (α Gal; an IFN γ inducer) was
366 injected into these mice. The levels of sALT activity and intrahepatic UPR-related molecule
367 expression were measured 24 hours after IFN α or α Gal treatment. As shown in Fig 8D,
368 sALT elevation was almost completely blocked in the tunicamycin pre-treated animals
369 compared to the vehicle-treated control group after IFN α (3665 \pm 500 U/L vs. 207 \pm 73 U/L,
370 p<0.001). Tunicamycin treatment also suppressed IFN γ -mediated liver injury in HBs-Tg
371 mice as tunicamycin treated mice showed up to a 6-fold reduction in sALT levels compared
372 to the controls after α Gal injection (Fig 8E; 12020 \pm 1100 U/L vs. 1940 \pm 388 U/L, p<0.001).
373 These data indicate that UPR augmentation rescues HBsAg accumulating cells from the
374 cytolytic effect of type I and type II IFNs. The data also suggest that IFN α and IFN γ utilize a
375 similar molecular mechanism to induce cell death in HBsAg accumulating hepatocytes (Fig
376 8F).

377 **Fig 8. UPR upregulation alleviates IFN-induced liver injury in HBs-Tg mice. (A)**

378 Experimental design to test the effect of GRP78 suppression on IFN-induced liver injury. (B)

379 sALT levels at 24 hours after IFN α injection in siGRP78 treated HBs-Tg mice compared

380 with controls. (C) Experimental design to test the effect of tunicamycin administration

381 (0.1mg/kg) on IFN-induced liver injury. IFN α (5 MU/kg) or α -Galactosylceramide (α Gal)

382 (50ng/mouse) were intravenously injected to HBs-Tg mice at 4 hours after tunicamycin

383 administration. The immunoblots below show the intrahepatic level of UPR markers at

384 indicated time points. (D) sALT levels at 24 hours after IFN α injection in tunicamycin
385 (TUN) treated HBs-Tg mice compared with controls. (E) sALT levels at 24 hours after α Gal
386 injection in tunicamycin and vehicle-treated HBs-Tg mice. Mean values +/- s.d of pooled
387 data from 3 independent experiments are shown. (F) A schema depicting our hypotheses on
388 the effect of IFN-1 signaling on UPR to induce ER stress-related cell death in HBsAg
389 accumulating hepatocytes.

390

391

392 **Discussion**

393 In this study, we examined whether and how IFNs induce liver injury in association
394 with HBsAg accumulation in the liver. IFN α directly and specifically induced cell death in
395 HBsAg accumulating hepatocytes in association with suppression of the pro-survival UPR.
396 IFN γ appears to use the same mechanism to cause cellular damage. Importantly, UPR
397 augmentation significantly reduced the cytolytic effect of IFNs on HBsAg accumulating
398 hepatocytes. Our data highlights an as yet unknown characteristic of the IFN signaling-UPR
399 axis that potentially presents important targets for regulating ER-stress associated cell death.

400 The HBV envelope consists of three closely related envelope proteins: small (S),
401 middle (M), and large (L), all of which have identical C-terminal ends [35]. The large
402 envelope protein (LHBs) is filamentous and tends to accumulate in the ER [36]. Lineage 107-
403 5D transgenic mice used in this study produce LHBs predominantly, and were shown to be
404 exquisitely sensitive to IFN γ [31,34,37,38]. IFN γ was also shown to induce cell death in
405 oligodendrocytes that accumulate MHC-1 heavy chains [39]. However, little is known about
406 the mechanism by which IFN γ induces cell death in ER stress-accumulating cells. In contrast,
407 the impact of type I IFNs on ER stress-accumulating cells had not been examined. Due to
408 intracellular pattern recognition receptors (PRRs) such as RIG-I, IFN α can be specifically
409 induced by virus-infected cells [3]. Less understood was whether and how IFN α specifically
410 targets virus-infected cells to exert its antiviral activity. Although many viruses are shown to
411 induce ER stress and UPR [14–19], the interaction between IFNs, ER stress, and UPR
412 remains largely unexplored. To our knowledge, this is the first study that demonstrates the
413 direct and specific cytotoxicity of IFN α on ER stress-accumulating cells.

414 Importantly, the suppressive effect of IFN on UPR was evident not only in HBs-Tg
415 mice (Fig 4) and HBV infected chimeric mice (Fig 5), but also on chemically induced UPR

416 (Fig 6D and 6E). IFN α suppressed the expression of phosphorylated and unphosphorylated
417 PERK, which is a key UPR molecule presumed to suppress protein synthesis [40]. In HBs-
418 Tg mice and HBV infected chimeric mice, IFN α also suppressed the expression of spliced
419 XBP1. XBP1 is a key transcription factor that binds to unfolded protein response elements
420 (UPRE) found in several genes encoding molecular chaperones and ER-associated
421 degradation (ERAD) [41]. IFN α did not suppress XBP1 in thapsigargin-treated PMHs. Of
422 note, thapsigargin treatment did not increase LDH in the supernatant, indicating that the
423 nature of ER stress caused by HBs-Tg mice and thapsigargin is very different. Previous
424 studies have shown that hepatic deficiency of PERK [42] or XBP1 [43,44] renders
425 hepatocytes hypersusceptible to ER stress-related cell death and disease. It is currently
426 unclear whether the suppression of these molecules is the primary cause triggering the
427 cascade of cell death after IFN treatment. Knockdown of the key UPR related molecules such
428 as XBP1 and PERK individually by siRNA did not induce cell death in the absence of IFNs.
429 It is possible that the simultaneous suppression of several UPR molecules or other unknown
430 factors induced by IFNs is required to initiate the cytolytic program. Alternatively, the
431 suppression of UPR by IFN signaling may be cytolytic only when GRP78 is highly
432 upregulated. Regardless, the current study demonstrated the detrimental effect of UPR
433 suppression on HBsAg accumulating hepatocytes.

434 GRP78 was upregulated after IFN treatment selectively in HBs-Tg mice, and its
435 upregulation was clearly associated with liver injury. Because GRP78 regulates the UPR
436 through direct interaction with ER stress sensors [45], it is reasonable that the upregulation of
437 GRP78 results in reduced UPR. Paradoxically, the main function of GRP78 is thought to
438 facilitate protein folding to reduce ER stress, and its expression is also induced by UPR
439 stimulation [46]. Ample evidence suggests the critical role of GRP78 in cancer cell survival
440 and proliferation. Site-specific deletion of GRP78 in the prostate epithelium suppresses

441 prostate tumorigenesis [47], and knockdown of GRP78 sensitizes various cancer cells to
442 chemotoxic, anti-hormonal, DNA damaging, and anti-angiogenesis agents [48]. In stark
443 contrast to these reports, more recent studies point to a pro-apoptotic role of GRP78
444 translocated to the cell surface. Ligation of a proapoptotic protein, prostate apoptosis
445 response-4 (Par-4), to GRP78 on cell surface induces apoptosis [49] . Experiments are
446 currently underway to test whether IFNs induce GRP78 translocation to the surface of
447 HBsAg accumulating hepatocytes.

448 CHOP does not seem to play a significant role in IFN α mediated cell death associated
449 with HBsAg accumulation in our setting (Fig 7B), although it was highly induced in direct
450 correlation with ALT elevation (Fig 4E). This observation appears to contradict the widely
451 accepted notion that CHOP sensitizes cells to ER stress-mediated death. For example, cells
452 lacking CHOP are significantly protected from the lethal consequences of ER stress [50,51].
453 However, mouse embryonic fibroblasts (MEFs) derived from CHOP-knockout mice exhibit
454 only partial resistance to ER stress-driven apoptosis [50]. Furthermore, liver-specific CHOP
455 knockdown had no impact on liver damage associated with urokinase plasminogen activator
456 (uPA) accumulation in the ER [52]. Thus, it is possible that the role of CHOP depends on the
457 organs and nature of ER stress.

458 Clinically, we do not know to what extent the observed phenomenon contributes to
459 the liver disease in HBV infected patients as HBV is a poor IFN-1-inducer [53]. However,
460 liver damage is one of the most common side effects of IFN α treatment [54]. In addition,
461 accumulating evidence suggests that ALT flares during chronic HBV infection are associated
462 with increases in serum IFN-1s [23,24]. Liver injury is often severe in CHB patients
463 superinfected with hepatitis C or hepatitis D viruses [55,56] , both of which induce IFN-1s.
464 While activated NK, NKT, and T cells have been assumed responsible for the liver injury
465 associated with IFNs [23,24], the current study newly identifies UPR downregulation as a

466 potential mechanism of IFN-mediated hepatotoxicity. One may argue that the levels of HBsAg
467 accumulation in the HBs-Tg mice cannot be attained in HBV infected patients. However,
468 some chronic hepatitis B patients, particularly those carrying HBV PreS1/PreS2 mutants [57–
469 59], exhibit ground glass hepatocytes (GGHs), a manifestation of HBsAg accumulation in the
470 ER, and tend to develop hepatic flares. Immune suppressed CHB patients occasionally
471 experience fibrosing cholestatic hepatitis, a severe form of hepatic flares, and exhibit GGHs
472 [20,21]. GGHs have been reported even in HBV-infected chimeric mice in association with
473 very high levels of intrahepatic HBV proteins and also mild hepatitis [60]. It is important to
474 point out that UPR was induced in HBV infected human hepatocytes in chimeric mice, and
475 UPR downregulation was observed in these mice after IFN α treatment, indicating that the
476 similar events observed in HBs-Tg mice could occur during bona fide HBV infection.

477 In conclusion, the results described herein suggest the previously unappreciated
478 mechanism by which IFNs selectively induces cell death in ER stress accumulating cells.
479 This mechanism may have evolved to selectively eliminate stressed cells due to virus
480 infections or other causes. On the other hand, the same mechanism potentially induces
481 chronic inflammation. Further studies are warranted to determine whether the IFN-UPR axis
482 contributes to the development of other ER stress-associated chronic inflammatory diseases,
483 such as alcoholic and non-alcoholic steatohepatitis, and neurodegenerative disorders.

484

485 **Materials and Methods**

486 **Ethics statement**

487 All experiments involving mice were performed in the Center for Experimental Animal
488 Science at Nagoya City University, following a protocol approved by the Institutional Animal

489 Care and Use Committee of the Nagoya City University Graduate School of Medical
490 Sciences (approved number: H30M_45).

491

492 **Mouse models and treatments**

493 Mouse care and experiments were performed at the Nagoya City University Center for
494 Experimental Animal Science following a protocol approved by the Institutional Animal Care
495 and Use Committee. Ten to twelve-week-old male mice were used in all the experiments.
496 HBV transgenic mice (Lineage 1.3.32) and HBs-Tg mice of the lineage 107-5D used in this
497 study were kindly provided by Dr. Francis V. Chisari. HBs-Tg mice produce filamentous
498 HBs proteins under the control of the albumin promoter, as previously described[27]. HBV-
499 Tg mice produce infectious Dane particles and HBV subviral particles as described
500 previously [28]. Human hepatocyte chimeric mice were generated by repopulating the livers
501 of severe combined immunodeficient mice transgenic for the urokinase-type plasminogen
502 activator gene (uPA^{+/+}/SCID^{+/+} mice) with human hepatocytes, and purchased from Phoenix
503 Bio Co., Ltd, (Hiroshima Japan). Chimeric mice were infected with HBV as previously
504 described¹⁵, and 3-4 mice/group subcutaneously received 25ng/g of pegylated-human
505 interferon α (Peg-hIFN α -2a) (Hoffmann La Roche, Basel, Switzerland). To activate IFN-1
506 signaling, poly I:C (Sigma) (10 μ g/mouse) was injected intravenously. To block type-1 IFN
507 signaling, 250 μ g anti-IFN α β R1 antibody (clone MAR1-5A3) or isotype control (IgG1)
508 (BioXcell, Lebanon, NH, USA) were injected intraperitoneally. To test the effect of IFN α , 5
509 million units per kg recombinant mouse IFN α (Miltenyi Biotec) were injected intravenously.
510 To upregulate UPR, 0.1mg/kg tunicamycin was injected intraperitoneally (Merck).

511

512 **Serum ALT and HBsAg analyses.**

513 Serum ALT was measured using the Dri-Chem 3500 analyzer according to the
514 manufacturer's instructions (Fuji, Tokyo, Japan). Serum HBsAg and intrahepatic HBsAg
515 were measured by a chemiluminescent enzyme immunoassay (CLEIA) using a
516 LumipulseG1200 analyzer (Fujirebio, Tokyo, Japan), as previously described [33].

517

518 **Detection of DNA fragmentation by TUNEL method.**

519 Mouse livers were perfused with PBS, harvested in Zn-formalin and transferred into 70%
520 ethanol 24 hours later. Tissue was then processed, embedded in paraffin and stained as
521 previously described [61]. In situ apoptosis detection was carried out by using a Terminal
522 deoxynucleotidyl transferase dUTP nick end labelling (TUNEL) apoptosis kit, according to
523 the manufacturer's instructions (ab206386; Abcam Biotechnology, Cambridge, UK). The
524 samples were counterstained with Mayer's hematoxylin for the morphological evaluation and
525 characterization of normal and apoptotic cells.

526

527 **Adoptive HBsAg-specific T cell transfer and In vivo HBsAg suppression.**

528 HBsAg-specific CD8⁺ T cells, derived from TCR transgenic mice (Env-28 specific, Lineage:
529 6C2.16) [62], were simulated in-vitro for one-week as previously described [31]. These cells
530 were intravenously injected into groups of HBs-Tg mice at a dose of 5×10^6 cells/mouse.
531 Groups of HBs-Tg mice were intravenously injected with a single dose (5mg/kg) cocktail of
532 HBV specific siRNA (si75, si251, si1803)[29,30,63] or Control siRNA complexed with a
533 pH-sensitive multifunctional envelope-type nanodevice (MEND) [29].

534

535 **Immunoblots**

536 Whole-cell extracts were obtained from liver tissue or cell pellets lysed in buffer (0.1%,
537 sodium dodecyl sulfate, 0.1% sodium deoxycholate, 1% IGEPAL) supplemented with
538 Protease and Phosphatase Inhibitor cocktails (Roche). Protein extracts were separated by
539 SDS-polyacrylamide gel electrophoresis then transferred onto polyvinylidene difluoride
540 (PVDF) membranes (Millipore, Temecula, CA). Primary antibodies and secondary antibodies
541 were used according to manufacturers' instructions. Primary antibodies used are GRP78
542 (#3177), CHOP (#2895), XBP1s (#12782), phospho-PERK (#3179) PERK (#3192), ISG15
543 (#2743) IRE1 α (#3294), Stat-1 (#9172), phospho-Stat-1 (#9167) (all from Cell Signaling
544 Technologies), GAPDH (abcam#8245), HBsAg (#5124A, Tokumen, Japan) phospho-IRE1 α
545 (Novus #NB100-2323) Detection was performed using the Immobilon Western
546 Chemiluminescent HRP Substrate (Millipore) and image capture was done using the A1680
547 imaging system (GE Healthcare).

548

549 **RNA extraction and gene expression analyses**

550 RNA was isolated from snap-frozen liver tissue obtained at selected time points using Isogen
551 (Nippon Gene, Tokyo, Japan) according to the manufacturer's instructions. For Microarray
552 analyses, 2 biological replicates for each selected time point were analyzed. Briefly, from
553 100ng total RNA, complementary RNA (cRNA) was prepared using the Low Input Quick-
554 Amp Labeling Kit, one color Cy3 protocol (Agilent Technologies, Santa Clara, CA, USA).
555 Purified labeled-cRNA and controls (Agilent One Color Spike-In Kit) were hybridized to
556 Agilent SurePrint G3 Mouse Gene Expression v2.0 Microarray Chips. Detection, data
557 extraction, and pre-analysis were performed using a G2505C Agilent microarray scanner,
558 Feature Extraction v10.10.1.1, and GeneSpring GX v14.8.0 software. Genes showing
559 differential kinetics between IFN treated or non-treated HBsAg and WT samples over the

560 period leading up to the onset of liver injury in HBs-Tg mice, i.e., 0, 2, 4, and 8 hour time
561 points, were identified using the time-course specific R program maSigPro [32]. Briefly,
562 maSigPro assesses the significance of the global model (i.e., if there are significant
563 differences with respect to time or treatment) and of each variable (i.e., which specific time
564 or treatment change is present) by fitting a regression model, considering time as a
565 continuous variable and creating specific variables for each treatment, thereby adjusting a
566 temporal profile for each time course. Genes significantly changed were selected and divided
567 into clusters of similar profiles for visualization of results. Microarray data have been
568 deposited into the NCBI Gene Expression Omnibus Repository (Accession # GSE 138916)
569 For microarray data validation and specific target gene expression analysis, quantitative real-
570 time polymerase chain reaction (qRT-PCR) was performed using the StepOnePlus Real-Time
571 PCR System (Applied Biosystems, Foster City, CA). From 2 μ g total RNA, complementary
572 DNA (cDNA) was synthesized using the High Capacity RNA-to-cDNA Kit (Applied
573 Biosystems). TaqMan Gene Expression Assay primer-probe sets used include; GRP78
574 (Mm00517690_g1, Hs00607129_gH), CHOP (Mm01135937_g1, Hs03834620_s1), XBP1s
575 (Custom), PERK (Mm00438700_m1, Hs00984006_m1), GAPDH (Mm99999915_g1,
576 Hs02758991_g1), IRE1 α (Mm00470233_m1), ISG15 (Mm01705338_s1, Hs01921425_s1),
577 IRF1(Hs00971960_m1) (all from Applied Biosystems). All qPCR data were normalized to
578 GAPDH.

579

580 **Isolation, culture, and treatment of primary mouse hepatocytes.**

581 Primary mouse hepatocytes were isolated from both HBs-Tg and their wildtype littermates
582 (controls) using a two-step protocol as previously described [62] with some modification.
583 Briefly, the liver was perfused with Liver Perfusion Medium (Gibco #17701) for 4 minutes at

584 a flow rate of 5ml/min followed by 0.8mg/ml Type 1 Collagenase (Worthington, UK) in
585 Dulbecco Minimum Essential Medium (Gibco # 11965-092) for 8-12 minutes at 5ml/min.
586 PMHs were cultured on Collagen 1 Biocoat 6-well plates (BD Biosciences) at a seeding
587 density of 1×10^5 cells/cm² in Hepatocyte Growth Medium with 2% DMSO. Thapsigargin
588 (5 μ M, Fujifilm-Wako, Osaka, Japan) was added to IFN α -treated WT-PMHs that were then
589 harvested after 6 and 12 hours. Recombinant mouse IFN α was added at 0.1MU/ml.
590 Recombinant mouse IFN γ was added at 0.01MU/ml per well.

591

592 **LDH activity assay.**

593 Cytotoxicity was measured by the release of lactate dehydrogenase (LDH) into the culture
594 media 72 hours after the addition of IFN α (final concentration, 0.1MU/ml). Collected
595 supernatants were assayed using the Dri-Chem analyzer according to the manufacturer's
596 instructions (Fuji, Tokyo, Japan). Data are presented as percentage specific cell lysis,
597 calculated as the ratio of the experimental LDH release (minus spontaneous release LDH) to
598 the maximum LDH release using 1% Triton-X (minus spontaneous release LDH) for each
599 plate.

600 % specific lysis = LDH [(experimental -spontaneous)/maximum lysis – spontaneous] x100

601

602 **Knockdown of UPR-related target genes.**

603 To suppress UPR related molecules in vivo and in vitro, the InvivoFectamine 3.0 and
604 Lipofectamine RNAiMAX transfection reagents were used respectively, together with siRNA
605 for the following targets; Control (#1), GRP78 (s607083, s67085), XBP1 (s76114), CHOP
606 (s64888), all according to manufacturer's instructions (all from Thermofisher Scientific).

607

608 **Statistics.**

609 Student's t-test and One-Way ANOVA were performed accordingly. Microarray data

610 bioinformatic analyses were performed as previously described [32]. Data are depicted as the

611 mean \pm SD, and P values < 0.05 were considered significant.

612

613

614 **Acknowledgements**

615 The authors are grateful to Dr. Francis V. Chisari (Scripps Research Institute) who produced

616 and provided the HBV and HBs-Tg mice used in this study and for his critical reading of the

617 manuscript. We also thank Takayo Takagi, Mayumi Hojo, and Kyoko Ito (Nagoya City

618 University, Japan) for their technical assistance.

619

620 **Author contributions**

621 Conceptualization: Masanori Isogawa

622 Data Curation: Ian Baudi, Masanori Isogawa, Federica Moalli, Masaya Onishi, and Keigo

623 Kawashima

624 Formal analysis: Masaya Onishi

625 Funding Acquisition: Masanori Isogawa, Takaji Wakita, Matteo Iannacone, and Yasuhito

626 Tanaka

627 Investigation: Ian Baudi, Masanori Isogawa, Federica Moalli, and Keigo Kawashima

628 Methodology: Ian Baudi, Masanori Isogawa, Federica Moalli, and Matteo Iannacone.

629 Resources: Yusuke Sato, Hideyoshi Harashima, Hiroyasu Ito, Tetsuya Ishikawa

630 Supervision: Masanori Isogawa, Yasuhito Tanaka

631 Writing – original draft: Ian Baudi, and Masanori Isogawa

632 Writing – review & editing: Ian Baudi, Masanori Isogawa, Federica Moalli, Masaya Onishi,

633 Keigo Kawashima, Yusuke Sato, Hideyoshi Harashima, Hiroyasu Ito, Tetsuya Ishikawa,

634 Takaji Wakita, Matteo Iannacone, and Yasuhito Tanaka

635

636 **Funding**

637 This research was supported by grants-in-aid from the Ministry of Education, Culture, Sports,

638 Science, and Technology, Japan, from the Japan Society for the Promotion of Science

639 (KAKENHI) under grants 17K09436 (M.I.) and 20K08313 (M.I.), and from the Research

640 Program on Hepatitis from the Japan Agency for Medical Research and Development

641 (AMED) under grants 19fk0310103h2003 (M.I.), 20fk0310103h2004 (M.I.), and

642 JP19fk0310101, JP20fk0310101 (Y.T.). The funders had no role in study design, data

643 collection and analysis, decision to publish, or preparation of the manuscript.

644

645 **Competing interests**

646 The authors have declared that no competing interests exist.

647 **References**

- 648 1. Samuel CE. Antiviral Actions of Interferons. *Clin Microbiol Rev.* 2001;14: 778–809.
649 doi:10.1128/CMR.14.4.778-809.2001
- 650 2. McNab F, Mayer-Barber K, Sher A, Wack A, O’Garra A. Type I interferons in
651 infectious disease. *Nat Rev Immunol.* 2015;15: 87–103. doi:10.1038/nri3787
- 652 3. Stetson DB, Medzhitov R. Type I Interferons in Host Defense. *Immunity.* 2006;25:
653 373–381. doi:10.1016/j.immuni.2006.08.007
- 654 4. Ron D, Walter P. Signal integration in the endoplasmic reticulum unfolded protein
655 response. *Nat Rev Mol Cell Biol.* 2007;8: 519–529. doi:10.1038/nrm2199
- 656 5. Hetz C. The unfolded protein response: controlling cell fate decisions under ER stress
657 and beyond. *Nat Rev Mol Cell Biol.* 2012;13: 89–102. doi:10.1038/nrm3270
- 658 6. Gerakis Y, Hetz C. Emerging roles of ER stress in the etiology and pathogenesis of
659 Alzheimer ’ s disease. 2018;285: 995–1011. doi:10.1111/febs.14332
- 660 7. Maiers JL, Malhi H. Endoplasmic Reticulum Stress in Metabolic Liver Diseases and
661 Hepatic Fibrosis. *Semin Liver Dis.* 2019;39: 235–248. doi:10.1055/s-0039-1681032
- 662 8. Lindholm D, Korhonen L, Eriksson O, Kõks S. Recent Insights into the Role of
663 Unfolded Protein Response in ER Stress in Health and Disease. 2017;5: 1–16.
664 doi:10.3389/fcell.2017.00048
- 665 9. Wang M, Kaufman RJ. The impact of the endoplasmic reticulum protein-folding
666 environment on cancer development. *Nat Rev Cancer.* 2014;14: 581–597.
667 doi:10.1038/nrc3800
- 668 10. Hetz C, Chevet E, Harding HP. Targeting the unfolded protein response in disease. *Nat*
669 *Rev Drug Discov.* 2013;12: 703–19. doi:10.1038/nrd3976
- 670 11. Yoshida H. ER stress and diseases. *FEBS J.* 2007;274: 630–658. doi:10.1111/j.1742-
671 4658.2007.05639.x
- 672 12. Walter P, Ron D. The unfolded protein response: From stress pathway to homeostatic
673 regulation. *Science (80-).* 2011;334: 1081–1086. doi:10.1126/science.1209038
- 674 13. Wu J, Kaufman RJ. From acute ER stress to physiological roles of the unfolded

- 675 protein response. *Cell Death Differ.* 2006;13: 374–384. doi:10.1038/sj.cdd.4401840
- 676 14. Tardif KD, Mori K, Siddiqui A. Hepatitis C Virus Subgenomic Replicons Induce
677 Endoplasmic Reticulum Stress Activating an Intracellular Signaling Pathway. *J Virol.*
678 2002;76: 7453–7459. doi:10.1128/jvi.76.15.7453-7459.2002
- 679 15. Tardif KD, Mori K, Kaufman RJ, Siddiqui A. Hepatitis C Virus Suppresses the IRE1-
680 XBP1 Pathway of the Unfolded Protein Response. *J Biol Chem.* 2004;279: 17158–
681 17164. doi:10.1074/jbc.M312144200
- 682 16. Zambrano JL, Ettayebi K, Maaty WS, Faunce NR, Bothner B, Hardy ME. Rotavirus
683 infection activates the UPR but modulates its activity. *Virology.* 2011;8: 359.
684 doi:10.1186/1743-422X-8-359
- 685 17. Perera N, Miller JL, Zitzmann N. The role of the unfolded protein response in dengue
686 virus pathogenesis. *Cellular Microbiology.* 2017. p. e12734. doi:10.1111/cmi.12734
- 687 18. Blázquez AB, Escribano-Romero E, Merino-Ramos T, Saiz JC, Martín-Acebes MA.
688 Stress responses in flavivirus-infected cells: Activation of unfolded protein response
689 and autophagy. *Frontiers in Microbiology.* 2014. pp. 1–7.
690 doi:10.3389/fmicb.2014.00266
- 691 19. Li S, Ye L, Yu X, Xu B, Li K, Zhu X, et al. Hepatitis C virus NS4B induces unfolded
692 protein response and endoplasmic reticulum overload response-dependent NF- κ B
693 activation. *Virology.* 2009;391: 257–264. doi:10.1016/j.virol.2009.06.039
- 694 20. Davies SE, Portmann BC, O’grady JG, Aldis PM, Chaggar K, Alexander GJM, et al.
695 Hepatic histological findings after transplantation for chronic hepatitis B virus
696 infection, including a unique pattern of fibrosing cholestatic hepatitis. *Hepatology.*
697 1991;13: 150–157. doi:10.1002/hep.1840130122
- 698 21. Lau JYN, Bain VG, Davies SE, O’Grady JG, Alberti A, Alexander GJM, et al. High-
699 level expression of hepatitis B viral antigens in fibrosing cholestatic hepatitis.
700 *Gastroenterology.* 1992;102: 956–962. doi:https://doi.org/10.1016/0016-
701 5085(92)90182-X
- 702 22. Lok ASF, McMahon BJ. Chronic hepatitis B. *Hepatology.* 2007.
703 doi:10.1002/hep.21513
- 704 23. Dunn C, Brunetto M, Reynolds G, Christophides T, Kennedy PT, Lampertico P, et al.

- 705 Cytokines induced during chronic hepatitis B virus infection promote a pathway for
706 NK cell-mediated liver damage. *J Exp Med.* 2007;204: 667–680.
707 doi:10.1084/jem.20061287
- 708 24. Tan AT, Koh S, Goh W, Zhe HY, Gehring AJ, Lim SG, et al. A longitudinal analysis
709 of innate and adaptive immune profile during hepatic flares in chronic hepatitis B. *J*
710 *Hepatol.* 2010;52: 330–339. doi:10.1016/j.jhep.2009.12.015
- 711 25. Deng G, Zhou G, Zhang R, Zhai Y, Zhao W, Yan Z, et al. Regulatory Polymorphisms
712 in the Promoter of CXCL10 Gene and Disease Progression in Male Hepatitis B Virus
713 Carriers. *Gastroenterology.* 2008;134: 716–726. doi:10.1053/j.gastro.2007.12.044
- 714 26. Wong GLH, Chan HLY, Chan HY, Tse CH, Chim AML, Lo AOS, et al. Serum
715 interferon-inducible protein 10 levels predict hepatitis B s antigen seroclearance in
716 patients with chronic hepatitis B. *Aliment Pharmacol Ther.* 2016;43: 145–153.
717 doi:10.1111/apt.13447
- 718 27. Chisari F V., Filippi P, Buras JON, McLachlan A, Popper H, Pinkert CA, et al.
719 Structural and pathological effects of synthesis of hepatitis B virus large envelope
720 polypeptide in transgenic mice. *Proc Natl Acad Sci.* 1987;84: 6909–6913.
721 doi:10.1073/pnas.84.19.6909
- 722 28. Guidotti LG, Matzke B, Schaller H, Chisari F V. High-level hepatitis B virus
723 replication in transgenic mice. *J Virol.* 1995;69: 6158–69. Available:
724 <http://www.ncbi.nlm.nih.gov/pubmed/7666518>
725 <http://www.pubmedcentral.nih.gov/articlerender.fcgi?artid=PMC189513>
- 726 29. Yamamoto N, Sato Y, Munakata T, Kakuni M, Tateno C, Sanada T, et al. Novel pH-
727 sensitive multifunctional envelope-type nanodevice for siRNA-based treatments for
728 chronic HBV infection. *J Hepatol.* 2016;64: 547–555. doi:10.1016/j.jhep.2015.10.014
- 729 30. Wooddell CI, Rozema DB, Hossbach M, John M, Hamilton HL, Chu Q, et al.
730 Hepatocyte-targeted RNAi therapeutics for the treatment of chronic hepatitis B virus
731 infection. *Mol Ther.* 2013;21: 973–985. doi:10.1038/mt.2013.31
- 732 31. Ando K, Moriyama T, Guidotti LG, Wirth S, Schreiber RD, Schlicht HJ, et al.
733 Mechanisms of class I restricted immunopathology. A transgenic mouse model of
734 fulminant hepatitis. *J Exp Med.* 1993;178: 1541–54. doi:10.1084/jem.178.5.1541

- 735 32. Conesa A, Talón M, Nueda MJ, Ferrer A. maSigPro: a method to identify significantly
736 differential expression profiles in time-course microarray experiments. *Bioinformatics*.
737 2006;22: 1096–1102. doi:10.1093/bioinformatics/btl056
- 738 33. Sugiyama M, Tanaka Y, Kato T, Orito E, Ito K, Acharya SK, et al. Influence of
739 hepatitis B virus genotypes on the intra- and extracellular expression of viral DNA and
740 antigens. *Hepatology*. 2006;44: 915–924. doi:10.1002/hep.21345
- 741 34. Gilles PN, Guerrette DL, Ulevitch RJ, Schreiber RD, Chisari F V. HBsAg retention
742 sensitizes the hepatocyte to injury by physiological concentrations of interferon- γ .
743 *Hepatology*. 1992;16: 655–663. doi:10.1002/hep.1840160308
- 744 35. Ito K, Qin Y, Guarnieri M, Garcia T, Kwei K, Mizokami M, et al. Impairment of
745 Hepatitis B Virus Virion Secretion by Single-Amino-Acid Substitutions in the Small
746 Envelope Protein and Rescue by a Novel Glycosylation Site. *J Virol*. 2010;84: 12850–
747 12861. doi:10.1128/JVI.01499-10
- 748 36. Ou JH, Rutter WJ. Regulation of secretion of the hepatitis B virus major surface
749 antigen by the preS-1 protein. *J Virol*. 1987;61: 782–786.
- 750 37. Ito H, Ando K, Ishikawa T, Saito K, Takemura M, Imawari M, et al. Role of
751 TNF- Produced by Nonantigen-Specific Cells in a Fulminant Hepatitis Mouse Model.
752 *J Immunol*. 2009;182: 391–397. doi:10.4049/jimmunol.182.1.391
- 753 38. Chen Y, Sun R, Jiang W, Wei H, Tian Z. Liver-specific HBsAg transgenic mice are
754 over-sensitive to Poly(I:C)-induced liver injury in NK cell- and IFN-gamma-dependent
755 manner. *J Hepatol*. 2007;47: 183–190. doi:10.1016/j.jhep.2007.02.020
- 756 39. Baerwald KD, Corbin JG, Popko B. Major histocompatibility complex heavy chain
757 accumulation in the endoplasmic reticulum of oligodendrocytes results in myelin
758 abnormalities. *J Neurosci Res*. 2000;59: 160–169. doi:10.1002/(SICI)1097-
759 4547(20000115)59:2<160::AID-JNR2>3.0.CO;2-K
- 760 40. Harding HP, Zhang Y, Bertolotti A, Zeng H, Ron D. Perk is essential for translational
761 regulation and cell survival during the unfolded protein response. *Mol Cell*. 2000;5:
762 897–904. doi:10.1016/S1097-2765(00)80330-5
- 763 41. Yoshida H, Matsui T, Yamamoto A, Okada T, Mori K. XBP1 mRNA is induced by
764 ATF6 and spliced by IRE1 in response to ER stress to produce a highly active

- 765 transcription factor. *Cell*. 2001;107: 881–891. doi:10.1016/S0092-8674(01)00611-0
- 766 42. Teske BF, Wek SA, Bunpo P, Cundiff JK, McClintick JN, Anthony TG, et al. The
767 eIF2 kinase PERK and the integrated stress response facilitate activation of ATF6
768 during endoplasmic reticulum stress. *Mol Biol Cell*. 2011;22: 4390–4405.
769 doi:10.1091/mbc.e11-06-0510
- 770 43. Liu X, Henkel AS, LeCuyer BE, Schipma MJ, Anderson KA, Green RM. Hepatocyte
771 X-box binding protein 1 deficiency increases liver injury in mice fed a high-fat/sugar
772 diet. *Am J Physiol Gastrointest Liver Physiol*. 2015;309: G965-74.
773 doi:10.1152/ajpgi.00132.2015
- 774 44. Olivares S, Henkel AS. Hepatic Xbp1 Gene Deletion Promotes Endoplasmic
775 Reticulum Stress-induced Liver Injury and Apoptosis *. 2015;290: 30142–30151.
776 doi:10.1074/jbc.M115.676239
- 777 45. Bertolotti A., Zhang Y., Hendershot L. HH and RD (2000). Dynamic interaction of
778 BiP and the ER stress transducers in the unfolded protein response. *Nature Cell Biol*.
779 2, 326–332..pdf. 2000;2.
- 780 46. Gething M-J. Role and regulation of the ER chaperone BiP. *Semin Cell Dev Biol*.
781 1999;10: 465–472. doi:<https://doi.org/10.1006/scdb.1999.0318>
- 782 47. Fu Y, Wey S, Wang M, Ye R, Liao C, Roy-Burman P, et al. Pten null prostate
783 tumorigenesis and AKT activation are blocked by targeted knockout of ER chaperone
784 GRP78/BiP in prostate epithelium. *Proc Natl Acad Sci U S A*. 2008;105: 19444–9.
785 doi:10.1073/pnas.0807691105
- 786 48. Lee AS. Glucose-regulated proteins in cancer: molecular mechanisms and therapeutic
787 potential. *Nat Rev Cancer*. 2014;14: 263. Available: <https://doi.org/10.1038/nrc3701>
- 788 49. Burikhanov R, Zhao Y, Goswami A, Qiu S, Schwarze SR. The Tumor Suppressor Par-
789 4 Activates an Extrinsic Pathway for Apoptosis. *Cell*. 2009;138: 377–388.
790 doi:10.1016/j.cell.2009.05.022
- 791 50. Zinszner H, Kuroda M, Wang X, Batchvarova N, Lightfoot RT, Remotti H, et al.
792 CHOP is implicated in programmed cell death in response to impaired function of the
793 endoplasmic reticulum. *Genes Dev*. 1998;12: 982–995. doi:10.1101/gad.12.7.982
- 794 51. Oyadomari S, Koizumi A, Takeda K, Gotoh T, Akira S, Araki E, et al. Targeted

- 795 disruption of the Chop gene delays endoplasmic reticulum stress-mediated diabetes. *J*
796 *Clin Invest.* 2002;109: 525–532. doi:10.1172/JCI200214550
- 797 52. Nakagawa H, Umemura A, Taniguchi K, Font-Burgada J, Dhar D, Ogata H, et al. ER
798 Stress Cooperates with Hypernutrition to Trigger TNF-Dependent Spontaneous HCC
799 Development. *Cancer Cell.* 2014;26: 331–343. doi:10.1016/j.ccr.2014.07.001
- 800 53. Wieland S, Thimme R, Purcell RH, Chisari F V. Genomic analysis of the host
801 response to hepatitis B virus infection. *Proc Natl Acad Sci U S A.* 2004;101: 6669–74.
802 doi:10.1073/pnas.0401771101
- 803 54. Perrillo R. Benefits and risks of interferon therapy for hepatitis B. *Hepatology.*
804 2009;49: S103–S111. doi:10.1002/hep.22956
- 805 55. Liaw Y-F, Chen Y-C, Sheen I-S, Chien R-N, Yeh C-T, Chu C-M. Impact of acute
806 hepatitis C virus superinfection in patients with chronic hepatitis B virus infection.
807 *Gastroenterology.* 2004;126: 1024–1029. doi:10.1053/j.gastro.2004.01.011
- 808 56. Negro F. Hepatitis D Virus Coinfection and Superinfection. *Cold Spring Harb Perspect*
809 *Med.* 2014;4: a021550–a021550. doi:10.1101/cshperspect.a021550
- 810 57. Sugiyama M, Tanaka Y, Kurbanov F, Maruyama I, Shimada T, Takahashi S, et al.
811 Direct Cytopathic Effects of Particular Hepatitis B Virus Genotypes in Severe
812 Combined Immunodeficiency Transgenic With Urokinase-Type Plasminogen
813 Activator Mouse With Human Hepatocytes. *Gastroenterology.* 2009;136: 652-662.e3.
814 doi:10.1053/j.gastro.2008.10.048
- 815 58. Pollicino T, Cacciola I, Saffiotti F, Raimondo G. Hepatitis B virus PreS/S gene
816 variants: Pathobiology and clinical implications. *J Hepatol.* 2014;61: 408–417.
817 doi:10.1016/j.jhep.2014.04.041
- 818 59. Fan YF, Lu CC, Chen WC, Yao WJ, Wang HC, Chang TT, et al. Prevalence and
819 significance of hepatitis B virus (HBV) pre-S mutants in serum and liver at different
820 replicative stages of chronic HBV infection. *Hepatology.* 2001;33: 277–286.
821 doi:10.1053/jhep.2001.21163
- 822 60. Meuleman P, Libbrecht L, Wieland S, De R, Habib N, Kramvis A, et al. Immune
823 Suppression Uncovers Endogenous Cytopathic Effects of the Hepatitis B Virus
824 Immune Suppression Uncovers Endogenous Cytopathic Effects of the Hepatitis B

- 825 Virus. *J Virol.* 2006;80: 2797–2807. doi:10.1128/JVI.80.6.2797
- 826 61. Bénéchet AP, De Simone G, Di Lucia P, Cilenti F, Barbiera G, Le Bert N, et al.
827 Dynamics and genomic landscape of CD8+ T cells undergoing hepatic priming.
828 *Nature.* 2019. doi:10.1038/s41586-019-1620-6
- 829 62. Isogawa M, Chung J, Murata Y, Kakimi K, Chisari F V. CD40 Activation Rescues
830 Antiviral CD8+ T Cells from PD-1-Mediated Exhaustion. *PLoS Pathog.* 2013;9: 1–16.
831 doi:10.1371/journal.ppat.1003490
- 832 63. Kawashima K, Isogawa M, Hamada-Tsutsumi S, Baudi I, Saito S, Nakajima A, et al.
833 Type I Interferon Signaling Prevents Hepatitis B Virus-Specific T Cell Responses by
834 Reducing Antigen Expression. *J Virol.* 2018;92. doi:10.1128/jvi.01099-18
- 835
- 836

837 **Supporting information**

838 **S1 Fig**

839 Reduction of intrahepatic HBsAg. (A) Experimental design. In vivo suppression of HBsAg
840 using siRNA. HBs-Tg mice were intravenously injected with mixed siRNA targeting HBV
841 (5mg/kg) then sacrificed at the specified time points. (B) The graph shows >10 fold reduction
842 in HBV mRNA levels by siHBV treatment. (C) HBsAg levels in HBs-Tg mice treated with
843 siHBV compared with control mice.

844

845 **S2 Fig**

846 (A) Baseline expression of UPR markers in non-treated 107-5D HBs-Tg mice. The
847 Immunoblots show the expression of UPR molecules like CHOP, XBP1 and GRP78 in non-
848 treated HBs-Tg mice compared with normal WT mice. (B) Serum ALT levels in non-treated
849 HBs-Tg mice compared with normal WT mice.

850

851 **S3 Fig**

852 Characterization of the baseline extracellular and intracellular HBsAg levels in non-treated
853 HBV infected chimeric, HBV-Tg and HBs-Tg mice. (A) A graph showing the serum HBsAg
854 levels between chimeric mice, HBV-Tg and HBs-Tg mice. (B) A graph showing the
855 intracellular HBsAg levels per μg of liver protein between chimeric mice, HBV-Tg and
856 HBs-Tg mice.

857

858 **S4 Fig**

859 IFN γ is directly cytotoxic to hepatocytes accumulating HBsAg. (A) Timeline showing how
860 primary mouse hepatocytes (PMHs) from both HBs-Tg and WT mice were isolated, plated,
861 and treated with either IFN γ , while monitoring cytotoxicity at the specified time points. (B)
862 The graph shows significant LDH increase in HBs-Tg derived PMHs 72 hours after IFN γ
863 addition. (C) The immunoblots show the effect of IFN-1 signaling on UPR-related proteins at
864 specified time points after IFN γ treatment.

865

Fig 1

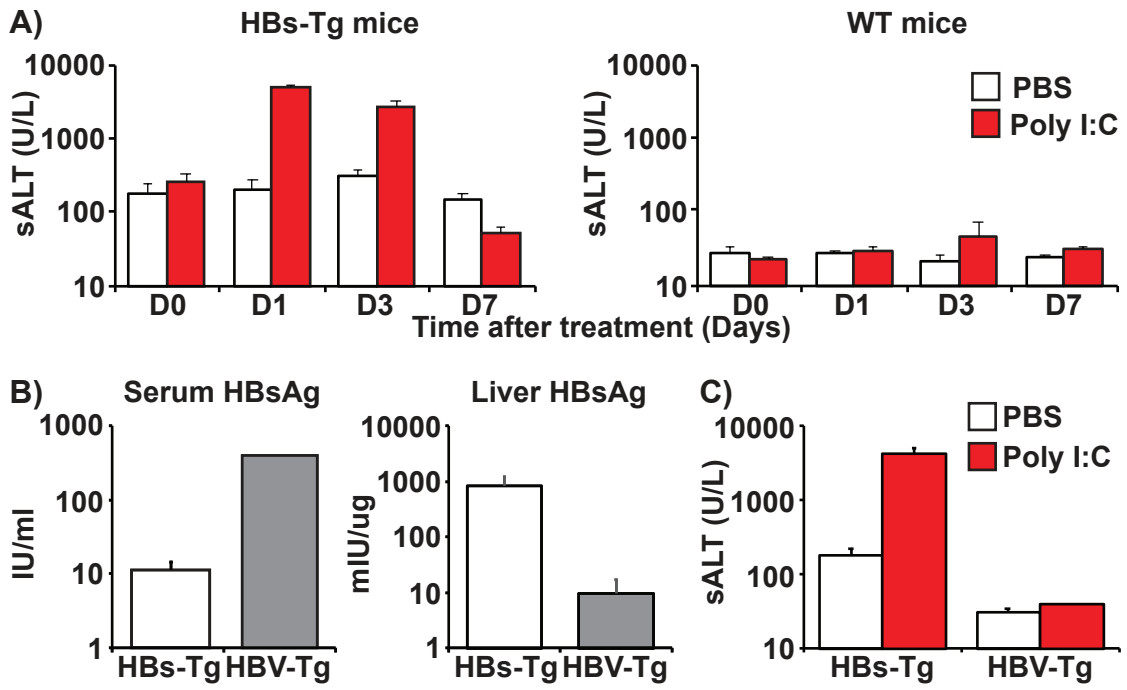


Fig 2

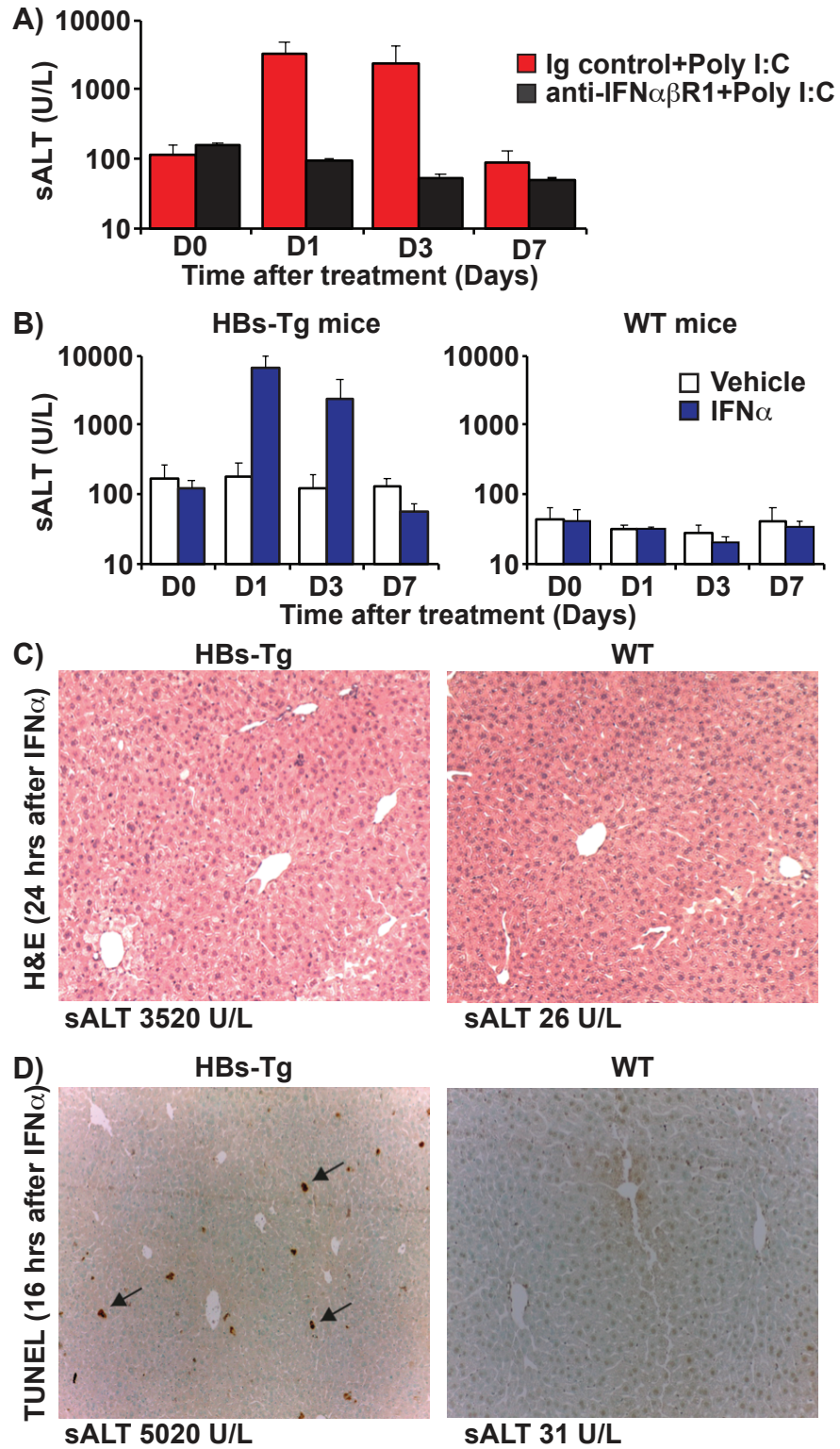
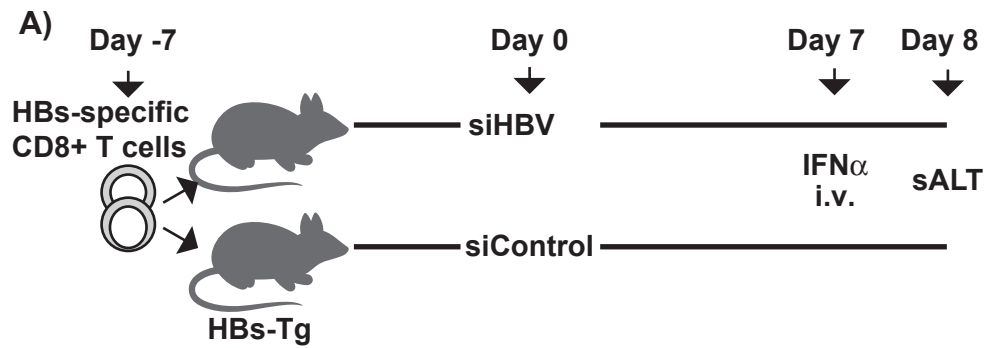
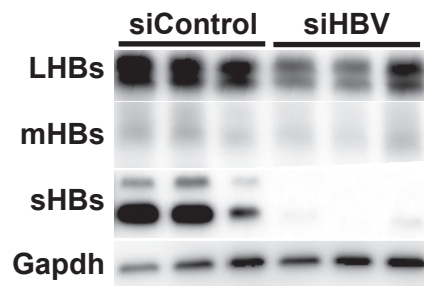


Fig 3



B) Intrahepatic HBsAg on Day 7



C)

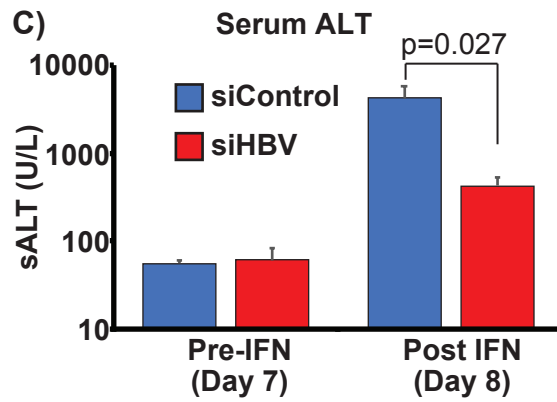


Fig 4

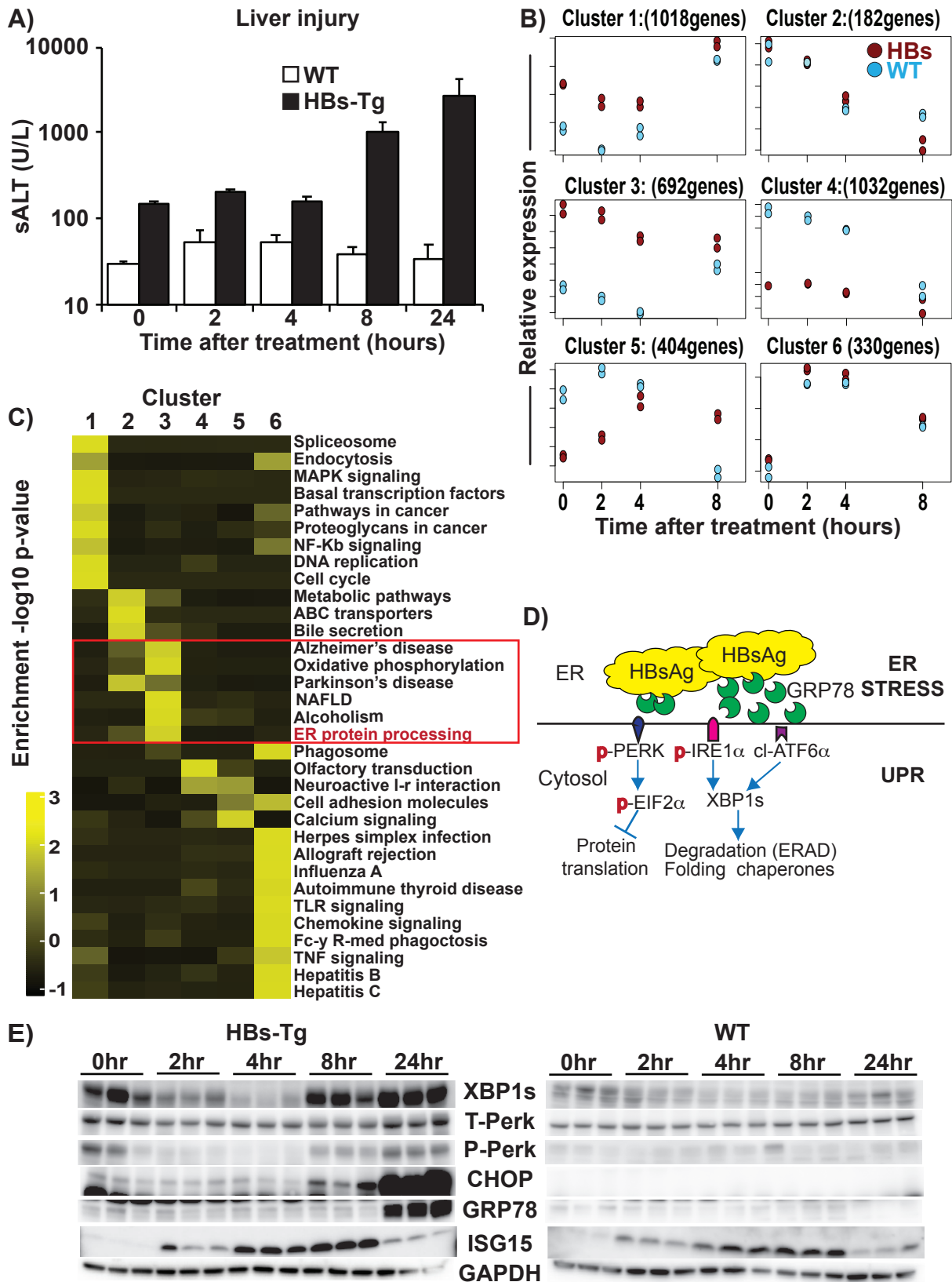


Fig 5

A) HBV infected human chimeric mice

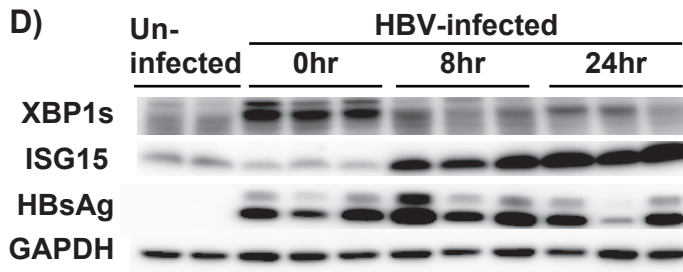
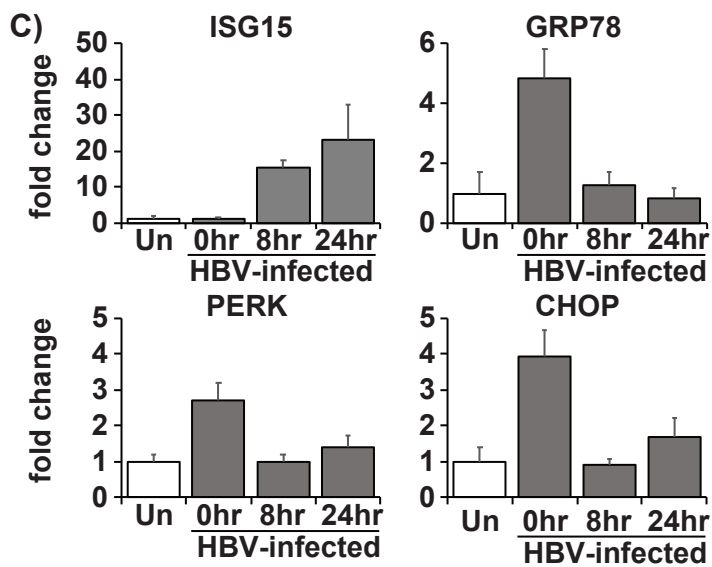
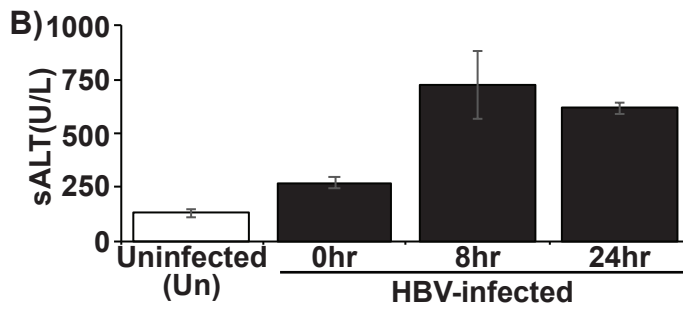
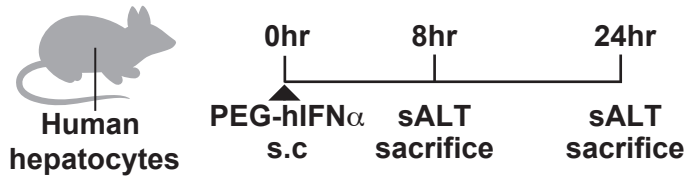


Fig 6

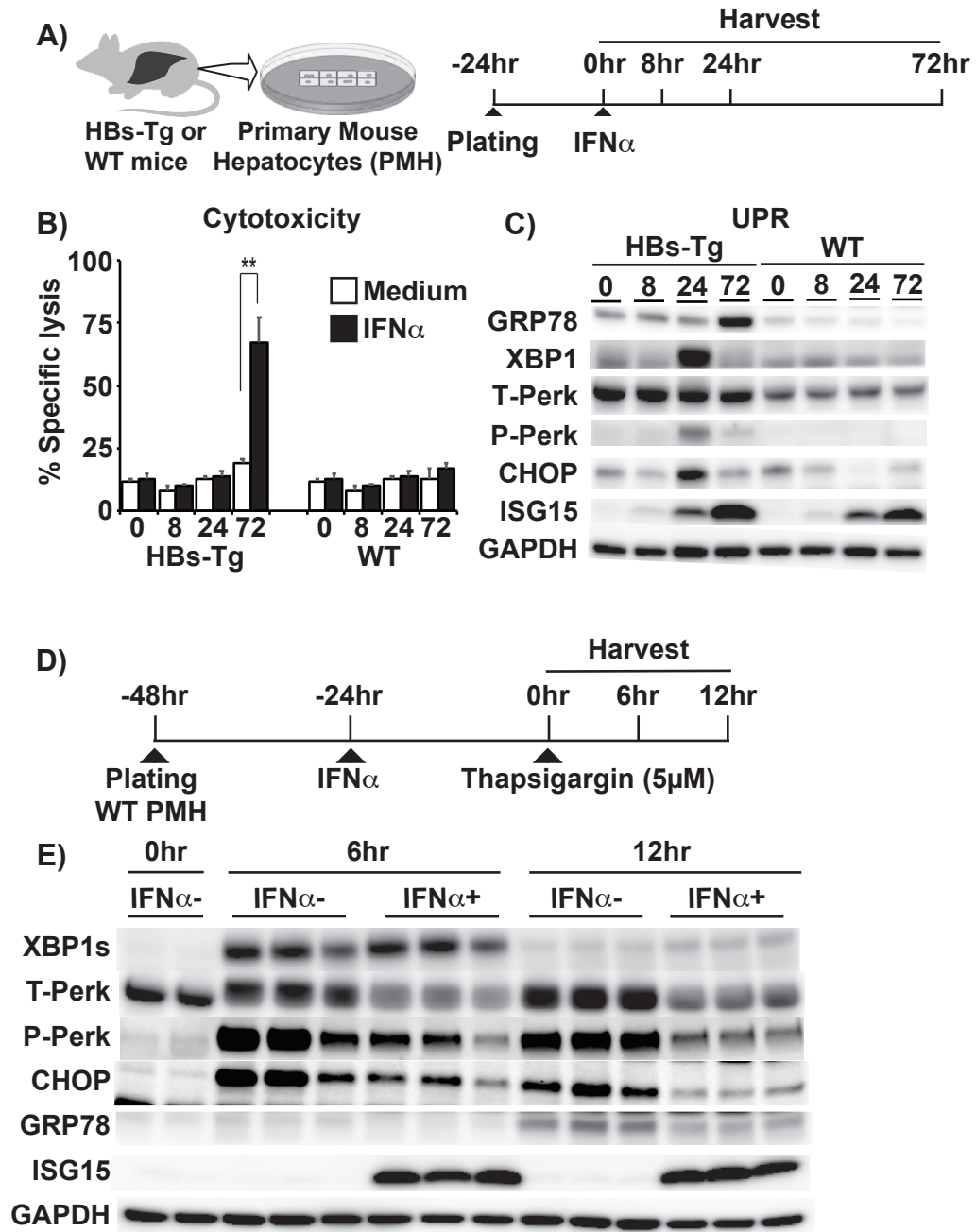


Fig 7

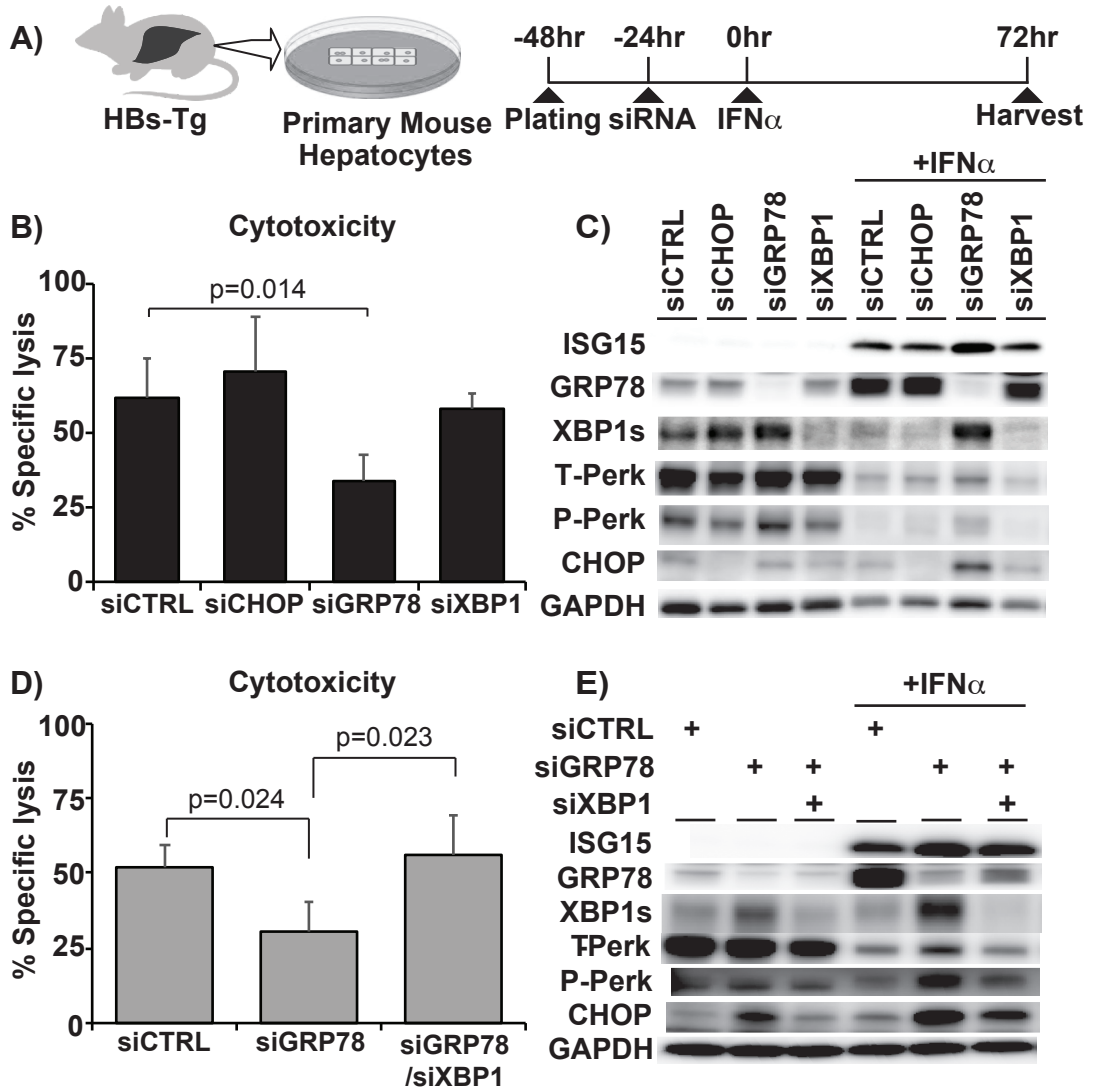
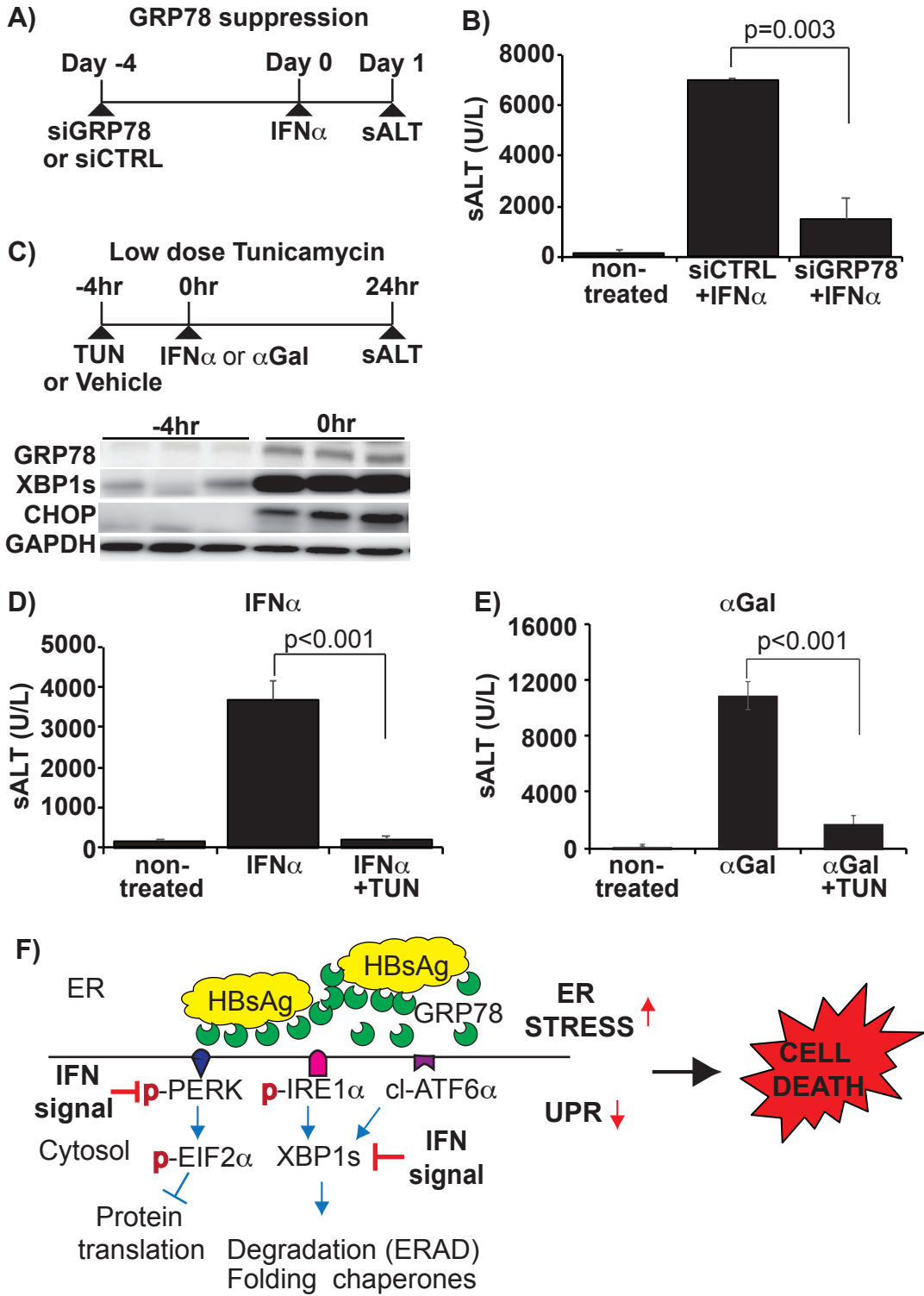
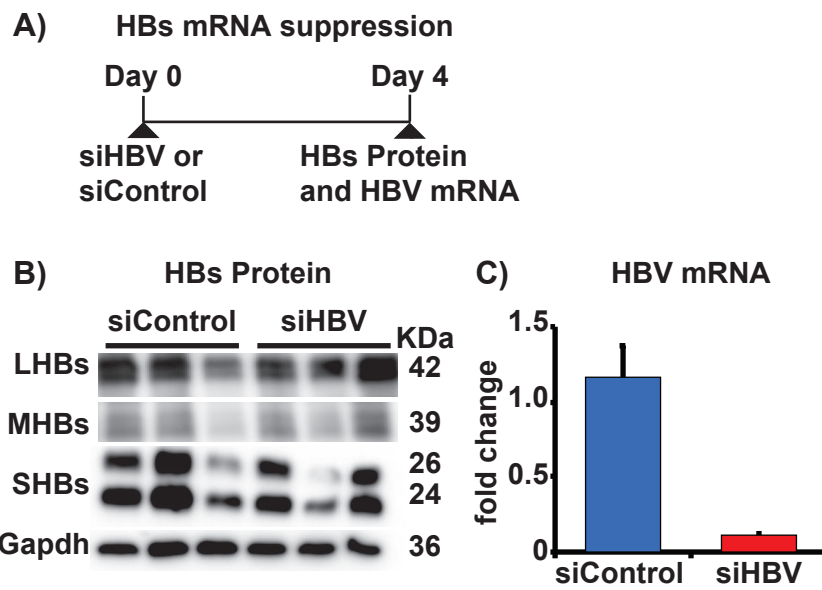


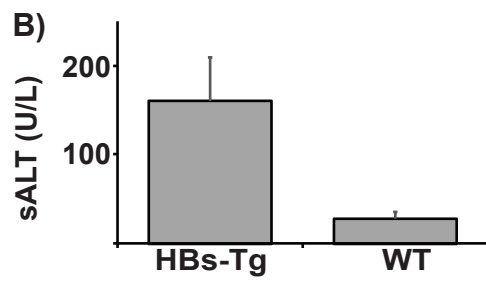
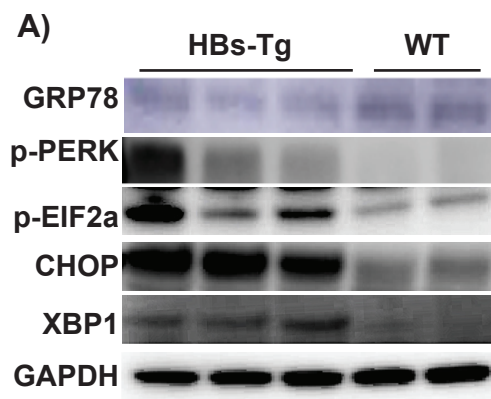
Fig 8



S1 Fig



S2 Fig



S3 Fig

